

COMMISSIONING OF THE 100 MEV PREINJECTOR HELIOS FOR THE SOLEIL SYNCHROTRON

A. Setty, D. Jousse, J-L. Pastre, F. Rodriguez, THALES, 92 704, Colombes, France
 A. Sacharidis, Euro MeV, Buc, France
 R. Chaput, J-P. Pollina, B. Pottin, M-A. Tordeux, SOLEIL, Saint-Aubin, France

Abstract

HELIOS is the 100 MeV electron linac pre-injector of SOLEIL the new French SR facility [1]. It has been supplied by THALES, as a turn-key system on the basis of SOLEIL APD design. The linac was commissioned in October 2005. This paper will remind the main features of the linac [2] especially on beam-loading compensation, and will give results obtained during the commissioning tests where a special care has been taken for emittance measurements. Specified and measured beam parameters will be compared to show the performance of the entire system.

INTRODUCTION

SOLEIL, the new French SR facility, has had the 100 MeV pre-injector installed and tested. The operational specifications of the linac are to be found in ref. [2]. The pre-injector is designed to work according to two operation modes: a Short Pulse Mode (2 ns – 0.5 nC) and a Long Pulse Mode (300 ns – 8 nC). For the two injection modes, the energy, energy spread, current, charge and emittance have been measured. Table 1 gives a summary of the commissioning measurements.

GENERAL DESCRIPTION OF THE LINAC

A detailed description can be found in ref. [1]. Fig. 1 shows the gun with the two 65l/s ion pumps.

The low energy part of the pre-injector is made up of a 90 kV triode gun, followed by the bunching components: a 3 GHz prebuncher and a standing wave bunching section. Four short focusing shielded lenses ensure the focusing between the gun and the buncher.

Two 4.5 m long, $2\pi/3$ travelling wave accelerating sections then increase the energy of the beam from 15 MeV at the exit of the buncher up to 100 MeV. The sections are used without external focusing, except for a triplet between them and a Glazer lens between the buncher and the first section.

The whole machine is powered by two 80 MW modulators that drive two 35 MW TH2100 klystrons. The RF output of the first klystron is split into two waveguides: one waveguide feeding the first accelerating section, while the second one feeding the bunching components. Final acceptance took place on the 15th of November 2005.



Figure 1: Gun with the ion pumps.

MEASUREMENTS

Diagnostics

Five FCT (Fast Current Transformers) and three fluorescent screens are available along the linac.

The principal linac parameters, energy, energy spread, charge and transverse emittance were measured using the diagnostics available along the transfer line between the linac and the booster ring.

The main components of the line were one FCT, two fluorescent screens, two charge monitors, an energy analysing slit, two bending magnets and an emittance monitor at the end of the straight branch.

Beam Optimisation Method

After the first 100 MeV beam on the 2nd of July 2005, the optimisation process was first carried out without feeding the second section. A small charge continuous beam (20 mA-86 ns), without modulation in the gun, was emitted in order to minimize the beam loading effect. At the linac exit the measured energy beam was 66 MeV and the total charge equal to 1.2 nC.

First stage: a beam with a phase extension of 20 degrees centred on the “wave crest” generates an energy spread band of 1.5%. This beam shifted by 40 degrees, with respect to the wave crest, induces an energy spread of 25.8%. This allows, with a bending magnet and two structures (buncher and analysing section), to give the phase extension and the temporal structure of the beam

Table 1 : Commissioning measurements in single and multi-pulse modes

	LPM		SPM		
	Specified	Measured	Specified	Measured	
Pulses				1	4
Pulse length (ns)	300	286	<2	1.3	1.3
Energy (MeV)	>=100	108	>=100	110	110
Charge/Pulse (nC)	8	9.3	0.5 and 2	0.52	2.15
Emittance (mm.mrad)					
Horizontal ($4\beta\gamma\sigma'$)	200	47	200	64	67
Vertical ($4\beta\gamma\sigma'$)	200	52	200	67	78
Energy spread (%)	± 1.5	± 0.5	± 1.5	± 0.58	± 0.82

with a precision of 1 degree at 3 GHz, i.e. a precision smaller than 1 picosecond.

Second stage: a frequency variation of the travelling wave section induces a phase shift with respect to the wave crest. A 50 kHz variation, i.e. a 1 degree temperature change of the cooling water of the section, induces a phase shift of 24 degrees between beam and RF field along the whole first structure, i.e. a mean value of 12 degrees.

If the section is warmed up, the frequency will be reduced with respect to the buncher frequency and the beam will get a phase advance while travelling across the section. If the section is cooled, the beam will be delayed.

In fact, with this method a 12 degrees phase shift was measured for a 1 degree temperature change of the cooling water.

The first stage gave, at the first section exit, a beam phase extension equal to 20 degrees (80% in 6 degrees) with a maximum density at 5 degrees with respect to the wave crest. At this stage, we were not able to conclude if the beam was advanced or delayed. The second stage confirmed the dynamics simulations by proving that it was a 5 degree phase advance.

The energy gain of the buncher was equal to 15 MeV with an input power of 5.5 MW and the first section gave 51 MeV for 11 MW. An input power of 8 MW in the second section, gave a 110 MeV beam at the linac exit.

The prebuncher increased the transmission at 15 MeV from 51% to 79% (55% to 83% simulated).

Current Transmission

Fig. 2 shows the FCT signals for the LPM mode. The commissioning has been done with a pulse length of 286 ns without any level decrease along the pulse. The specified value of 300 ns or more has been achieved easily. Fig. 3 shows the FCT signals for the 4 pulses of the SPM mode. The delay between 2 pulses was equal to 50 ns. A gun current level decrease of 4.5% was observed over the 4 pulses. The current's decrease was under 2% at the exit of the first section.



Figure 2: Beam transmission for the LPM mode.

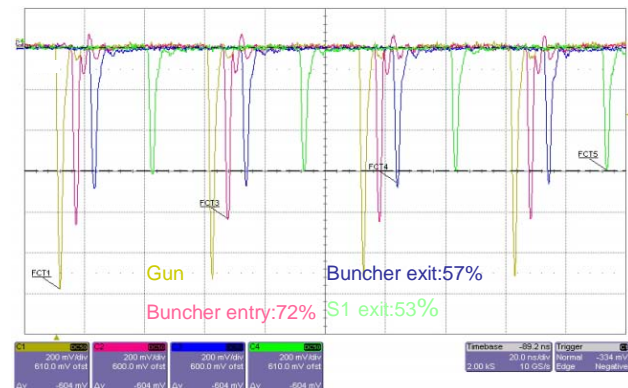


Figure 3: Beam transmission for the SPM mode.

Beam Loading Compensation

Generally, the first electrons of a long pulse have the greatest energy gain while crossing an accelerating section as the stored energy left for the last electrons is reduced. This is what we call the beam loading effect.

The beam loading compensation is achieved by sending the beam during the filling time of the second accelerating structure. In fact, the first electrons cross the last part of

the section without the nominal stored energy in it. The last electrons cross a full stored energy section. In certain conditions of power, charge and pulse length, the beam loading effect can be considerably reduced.

Fig. 4 shows the RF input and output signals of the second section together with the beam pulse.

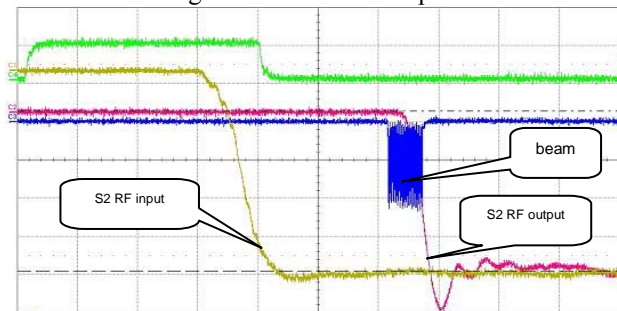
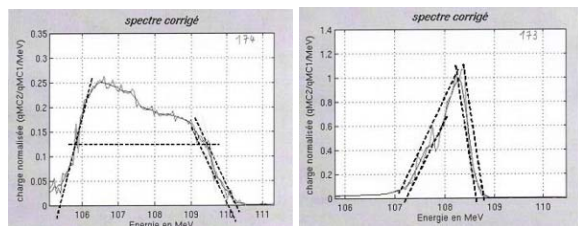


Figure 4: Beam loading compensation.

Energy Spread

The energy spread measurement was performed using the bending magnet together with the two charge monitors. The analysing slit was set at 0.25% resolution.

Fig. 5 and fig. 6 show the energy spread without and with beam loading compensation respectively. Fig. 7 shows the 2 curves put together at the same scale.



Without compensation With compensation
Figures 5 and 6: Energy spread.

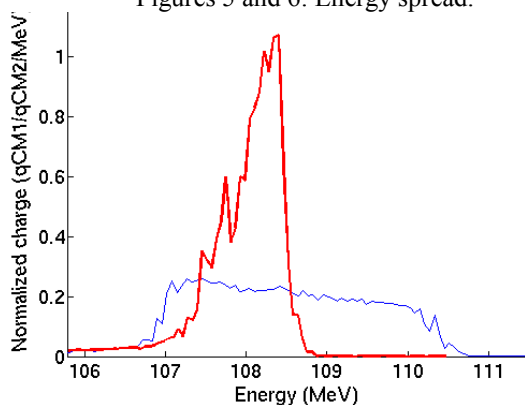


Figure 7: Energy spread for both cases.

The FWHM energy spread has been reduced from 3.75 MeV to 0.77 MeV for the 9.3 nC behind the slit.

Without the beam loading compensation and for the single pulse beam, the energy spread curve has a similar shape to the one in fig. 6. The FWHM band is equal to 0.58 MeV but for a 0.52 nC charge beam.

It can be seen from the commissioning results in table 1 that the energy spread of the short pulse with 0.52 nC is

larger than the energy spread of the 9.3 nC beam with the beam loading compensation.

Emittance

A detailed description can be found in ref. [3]. The emittance measurements were performed by varying the strength of a quadrupole and measuring the resulting variation of the beam size at a downstream Cerium doped YAG screen. A least square fitting routine was written to determine the emittance and the associated Twiss parameters that characterise the electron beam.

Fig. 8 shows the comparison between the simulations and the emittance measurement versus the gun current.

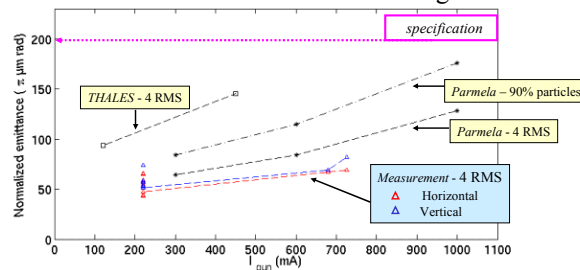


Figure 8: Comparison simulation-measurement.

The emittance at the gun level was overestimated in order to include the grid effect. Without the prebuncher, the mean emittance growth was around 50%. Without the Glazer lens or the triplet, the transmitted beam has been reduced by 3%, with no change of the emittance values.

After the commissioning, on the 16th of February 2006, for a LPM beam of 10 nC the normalized emittance was measured equal to 34 and 43 mm.mrad ($4\beta\gamma\sigma'$).

CONCLUSION

The SOLEIL pre-injector was successfully installed and commissioned during the past year. The measured linac parameters fitted well with the beam dynamic simulations.

Emittance growth was kept moderate by the special care that was taken on the gun design, to avoid an over-focusing outcoming beam and by the adjustment of the magnetic field between the gun and the buncher.

The expected low energy spread was achieved, thanks to the small phase extension at the buncher exit and to the use of the beam loading compensation.

The measured energy spread and emittance bettered the guaranteed values by at least a factor of three.

REFERENCES

- [1] B. Pottin and al., "HELIOS the linac injector of SOLEIL: installation and first results", PAC05, Knoxville, May 16-20 2005.
- [2] A. Setty, "Electrons beam dynamics of the 100MeV preinjector HELIOS for the SOLEIL synchrotron", EPAC'04, Switzerland, Lucerne, July 2004.
- [3] M-A. Tordeux and al., "Metrology for the beam emittance of the SOLEIL injector", this conference.